Shock-Tube Study of the Induction-Period Kinetics of the Hydrogen-Oxygen Reaction

Casimir J. Jachimowski and William M. Houghton

National Aeronautics and Space Administration, Langley Research Center, Hampton, Virginia, U.S.A.

The induction-period kinetics of the hydrogen-oxygen reaction has been investigated behind shock waves, using an ultraviolet line absorption technique to monitor the growth of the OH concentration. Rate coefficient data were obtained for the chain-branching reactions $H + O_2 \rightarrow OH + O$ and $O + H_2 \rightarrow OH + H$ in the temperature range 1200–1800°K. These are given in Arrhenius form by $k_2 = 9.9 \times 10^{13} \exp\left(-\frac{15020}{RT}\right)$ and $k_3 = 7.5 \times 10^{13} \exp\left(-\frac{11100}{RT}\right)$ liter mole^{-1} sec^{-1}. The expression for k_2 is in good agreement with the high and low-temperature values reported in the literature. The expression for k_3 yields values which are higher than those found in most of the literature but are in good agreement with some of the more recent data.

Introduction

When gaseous mixtures of hydrogen, oxygen, and argon are suddenly heated, for example by means of a shock wave, ignition is preceded by a short induction period. During the induction period the concentrations of the free radicals H, O, and OH grow rapidly by chain branching at essentially constant temperature and pressure with negligible depletion of reactants. The mechanism of the hydrogen-oxygen reaction during the induction period has been studied quite extensively [1–4], and it has been fairly well established that after a short initiation period during which small concentrations of atoms and radicals (H, O, OH) are produced the dominant reactions are as follows:

$$OH + H_2 \rightarrow H_2O + H \qquad (I)$$

$$H + O_2 \rightarrow OH + O \qquad (II)$$

$$O + H_2 \rightarrow OH + H \qquad (III)$$

with the reaction

$$H + O_2 + M \rightarrow HO_2 + M \qquad (IV)$$

also included at pressures greater than 1 atm and temperatures below about 1200°K. Calculations have shown that the growth of the free-radical concentrations during most of the induction period is exponential [5], exhibiting the simple time dependence

$$[x] = [x]_0 e^{\lambda t}, \quad x_i = H, O, OH \qquad (1)$$

where the subscript 0 refers to a pseudoinitial concentration. The exponential growth parameter, λ, is greatly influenced by the rates of the reactions that are dominant during the

Combustion & Flame, 15, 125–132 (1970)

induction period. Kondratiev [6] and Brokaw [7] have shown that under conditions where reaction IV can be neglected λ is the positive root of the cubic equation

$$\lambda^3 + a\lambda^2 + b\lambda - c = 0 \qquad (2)$$

where $a = k_1[H_2]_0 + k_2[O_2]_0 + k_3[H_2]_0$; $b = k_1k_3[H_2]_0^2$; $c = 2k_1k_2k_3[H_2]_0^2[O_2]_0$.

The purpose of this study was to measure the exponential growth parameter from the growth of OH concentration in shock-heated dilute mixtures of H_2 and O_2 in argon and to obtain kinetic data on the chain-branching reactions from Eq. 2. The concentration of the hydroxyl radical was determined by uv absorption spectroscopy, and the exponential growth parameter was determined from the OH concentration profile. Using the data from experiments performed at different $[H_2]:[O_2]$ ratios, we were able to obtain values for both k_2 and k_3 over the temperature range 1200–1800°K. The experiments were carried out under conditions where we considered the effect of reaction IV not to be significant.

Experimental Apparatus and Procedure

All the data were obtained behind incident shock waves in a 8.9-cm-i.d. stainless steel shock tube. The tube has a 214-cm-long driver section and a 580-cm-long driven section. Mylar diaphragms clamped between the driver and driven sections were ruptured by increasing the pressure in the driver section beyond their yield strength. Helium-nitrogen gas mixtures served as the driver gas. The speed of the shock wave was measured with a raster system upon which timing marks were superimposed at 10-μsec intervals. Test gas mixtures were prepared by the method of partial pressures from commercial hydrogen (99.9%), dry oxygen (99.6%), and argon (99.995%) without further purification.

For the measurement of OH concentration profiles a water-cooled lamp of Hinterreger design, powered by a 100-W, 28-MHz radio-frequency oscillator, was used. Maximum lamp intensity was obtained by using argon as the carrier gas at a pressure of 3.5 torr, with just a trace amount of water vapor continuously flowing through the discharge capillary. As a result of the low operating pressure and temperature the lamp generated sufficiently narrow lines so that the peak absorption technique [8, 9] could be used to compute concentration from the measured absorption. Radiation from the lamp was made parallel before entering the shock tube, and the emerging light was focused on a half-meter Czerny Turner type monochromator with a 1200 line mm^{-1} grating blazed at 3000 Å. The monochromator was set to pass six lines from the Q_1 branch and two lines from the P_1 branch. The region selected by the monochromator contains the $Q_1(1)$–$Q_1(6)$ lines and the $P_1(1)$ and $P_1(2)$ lines. Although other lines are also present in this region, the ones mentioned contribute more than 99% of the recorded light.

A quantitative relationship between absorbance and OH concentration was obtained by using $f_{00} = 8.45 \times 10^{-4}$ as the value for the rotationless oscillator strength and $a = 250\,(P/T)$, with P in atmospheres and T in K, as the damping constant expression. Details of the calibration procedure and its application to the rf-powered lamp are described elsewhere [9].

The light from the exit slit of the monochromator was detected by a photomultiplier, and the resulting signal was fed to an oscilloscope. The sweep of the oscilloscope was triggered by a signal from a platinum resistance gauge located 49.6 cm from the observation point. The sweep speeds and the delay generator of the oscilloscope were periodically calibrated with a timing mark generator. The transit time of the incident shock past the window was less than 2 μsec. The time constant of the recording equipment was better than 2 μsec for all the experimental runs.

We conducted experiments with four different gas mixtures whose compositions are given in Table 1. Initial test gas pressures varied from 10 to 40 mm Hg. The experimental temperature

Table 1. Composition of Experimental Mixtures

Mixture No.	H_2 %	O_2 %	Ar %
1	3.00	3.00	94.0
2	3.00	1.00	96.0
3	1.00	3.00	96.0
4	1.00	5.00	94.0

range extended from about 1200 to 1800 K. The pressure behind the shock wave varied between 0.25 and 0.75 atm. The data obtained in each run consisted of the recorded initial conditions, the shock velocity contained in the photograph from the raster oscilloscope, and the absorption trace contained on the oscilloscope photograph of the photoelectric signal. The shock waves showed no attenuation within the accuracy of the velocity measurements. The state parameters of the shock-heated gas immediately behind the shock front were calculated by a standard iterative technique, assuming frozen chemistry and full equilibrium of internal degrees of freedom. The temperature and pressure during the induction period were taken to be the same as those calculated just behind the shock front.

Data on the absorption by OH as a function of time were read from oscillograms such as Fig. 1 with an optical comparator. The signal-to-noise ratio of this absorption trace is characteristic of that obtained for all runs. The absorption data were reduced to concentration of OH and plotted on semilog paper. A straight line was hand-drawn through the data points, and an exponential growth parameter was calculated from the slope of the line (Fig. 2). Times measured from the oscillograms were multiplied by the density ratio across the shock front to convert to true reaction time.

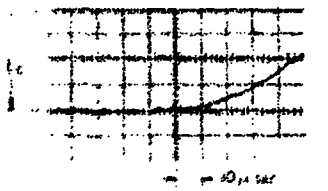

Figure 1. OH absorption curve for a 3:3:94 gas mixture. $T = 1294$ K, $[M] = 3.43 \times 10^{-5}$ mole liter^{-1}.

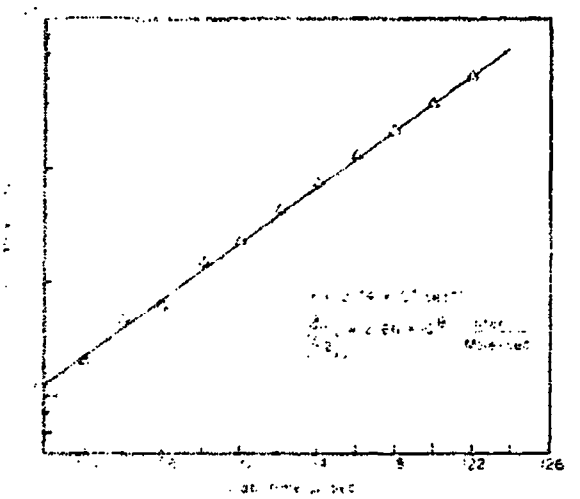

Figure 2. OH concentration profile for a 3:3:94 gas mixture. $T = 1294$ K, $[M] = 3.43 \times 10^{-5}$ mole liter^{-1}.

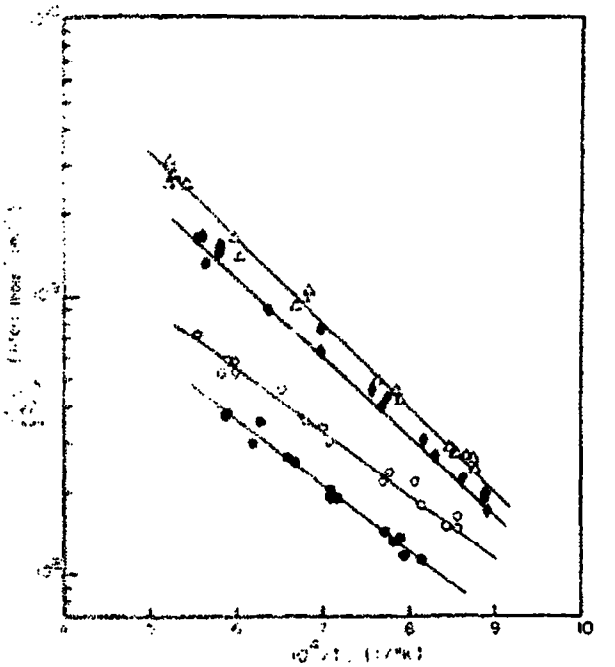

Figure 3. Plots of exponential growth parameter data, showing the dependence of $\lambda_1[O_2]_0$ on temperature and H_2:O_2 ratio. △, $H_2:O_2 = 4.0$; ■, $H_2:O_2 = 1.0$; ○, $H_2:O_2 = 0.25$; ●, $H_2:O_2 = 0.125$.

Results and Discussion

The results of the experiments are assembled in Table 2 and plotted in Fig. 3, where the ratio of the exponential growth parameter to the concentration of oxygen just behind the shock front is plotted against $1/T$. The function $\lambda/[O_2]_0$ is plotted because at low pressures, where reaction IV is not very significant, this function is independent of density and depends only on the values of the rate coefficients for reactions I, II, and III, and the ratio $[H_2]_0/[O_2]_0$. The results presented in Fig. 3 demonstrate the expected linear relationship between $\log \lambda/[O_2]_0$ and $1/T$, and the dependence of $\lambda/[O_2]_0$ at a given temperature on the ratio $[H_2]_0/[O_2]_0$. The curves drawn through the data points are least-square fits obtained by using a linear relationship between $\log \lambda/[O_2]_0$ and $1/T$.

The analysis of the data was based on fitting computed growth parameters to the experi-

Table 2. Experimental Results

T, K	$\lambda/[O_2]_0 \times 10^{-9}$, liter mole^{-1} sec^{-1}	$[M] \times 10^5$, mole liter^{-1}
	Mixture 1	
1840	2.43	3.75
1900	2.54	1.89
1890	2.78	1.89
1900	3.10	1.89
1830	2.50	1.87
1665	1.60	1.84
1649	1.41	1.83
1469	0.980	3.58
1460	1.06	3.57
1490	0.909	3.58
1268	0.452	6.88
1310	0.481	6.66
1265	0.413	6.88
1180	0.279	6.63
1160	0.267	6.54
1185	0.272	6.63
1140	0.256	6.66
1149	0.263	6.02
1140	0.228	6.68
1705	1.44	1.89
1705	1.51	1.89
1775	1.30	1.86
1780	1.61	1.88
1790	1.61	1.88
1564	0.855	1.83
1431	0.606	1.80
1431	0.775	1.80
1289	0.443	3.50
1300	0.400	3.50
1311	0.476	3.51
1204	0.266	3.43
1219	0.308	3.44
1155	0.219	5.09
1118	0.188	6.72
1118	0.159	6.72
1124	0.185	6.73
	Mixture 3	
1802	0.730	1.88
1709	0.521	1.86
1690	0.595	3.70
1655	0.532	3.68
1655	0.585	3.68
1537	0.363	3.63
1475	0.345	3.59
1430	0.331	1.78
1415	0.292	3.56
1300	0.213	3.48
1292	0.230	3.47
1185	0.145	6.77
1165	0.146	6.74
1165	0.161	6.74
1228	0.175	3.43
1241	0.211	3.44
	Mixture 4	
1230	0.110	7.12
1275	0.130	7.18
1266	0.134	7.18
1261	0.115	7.15
1295	0.139	7.20
1415	0.195	3.68
1415	0.188	3.69
1403	0.185	3.67
1492	0.257	1.87
1515	0.265	1.88
1610	0.294	2.86
1684	0.380	1.93
1700	0.372	1.93
1590	0.373	1.90

mental growth parameters. Substituting $\lambda = \lambda'[O_2]_0$ and $[H_2]_0 = x[O_2]_0$ in Eq. 2 gives

$$\lambda'^3 + (2xk_1 + k_2 + xk_3)\lambda'^2 + x^2k_1k_3\lambda' - 2x^2k_1k_2k_3 = 0 \quad (3)$$

This function was used in a generalized least-squares program [10] designed to obtain the values of the rate coefficients that make the computed growth parameters most closely approximate the experimental data for all $[H_2]_0/[O_2]_0$ ratios. Computations of this sort were made over the temperature range 1200–1800°K at a sequence of $1/T$ points, using values of λ' from each curve in Fig. 3. After numerous attempts it became obvious that the least-square procedure could not arrive at unique values for k_1, k_2, and k_3. We determined that this was due to the relative insensitivity of the data to reaction 1; consequently the rate coefficient k_1 in Eq. 3 is rather poorly defined by the data. Therefore we had to assume some values for k_1 in order to obtain values for k_2 and k_3. Values for k_1 were taken from the expression $k_1 = 2.3 \times 10^{10} \exp\left(-\frac{5200}{RT}\right)$ liter mole^{-1} sec^{-1}, reported by Dixon-Lewis, Wilson, and Westenberg [11], which we consider to be the "best" literature value available for the temperature range of our work.

When fitting the calculated exponential growth parameters to the experimental data, we also examined the sensitivity of the calculated values for k_2 and k_3 to the value used for k_1. This was done by varying the k_1 values of Dixon-Lewis et al. by ±50%. The values for k_2 were found to be rather insensitive to the value used for k_1. The extreme values for k_2 did not differ from each other by more than 5%. The values for k_3, on the other hand, were found to be rather sensitive to the value used for k_1. In this case the extreme values for k_3 differed from each other by about 40%. However, it was found that the computed growth parameters did not match the experimental values very well for the 1% H_2-8% O_2-91% Ar gas mixture, especially at the higher temperatures, when the k_1 values were varied. The best fit to the experimental data was achieved by using the k_1 expression of Dixon-Lewis etal. The values for k_2 and k_3 calculated at each $1/T$ calculated at each $1/T$ point were fit to Arrhenius rate coefficient expressions in the temperature range 1200–1800°K and are given by

$$k_2 = 9.9 \times 10^{10} \exp\left(-\frac{15020}{RT}\right) \text{liter mole}^{-1} \text{sec}^{-1} \quad (4)$$

$$k_3 = 7.5 \times 10^{10} \exp\left(-\frac{11100}{RT}\right) \text{liter mole}^{-1} \text{sec}^{-1} \quad (5)$$

By assigning a ±10% uncertainty in λ', we estimated the error in k_2 to be about ±15% and the error in k_3 to be about ±30%. The exponential growth parameters computed from the above rate coefficients are compared with experimental data in Fig. 4. The curves drawn through the experimental data in this figure were generated by solving Eq. 3 for λ', using the k_2 and k_3 obtained in this study and the k_1 values of Dixon-Lewis etal. Equations 4 and

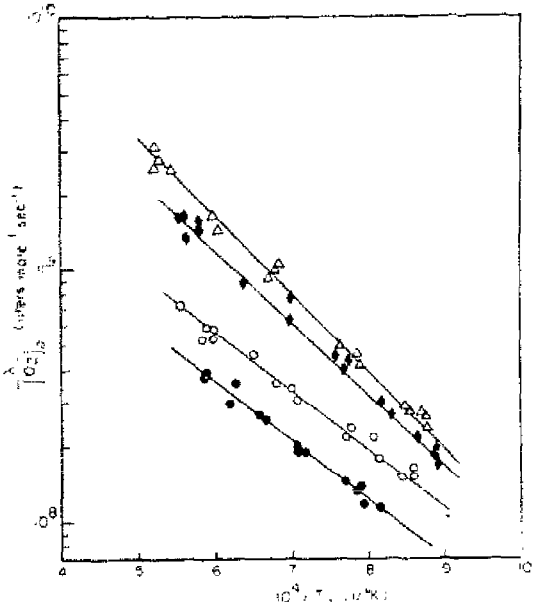

Figure 4. Calculated exponential growth parameter curves, giving the best fit to the experimental data. △, $H_2:O_2 = 4.0$; ■, $H_2:O_2 = 1.0$; ○, $H_2:O_2 = 0.25$; ●, $H_2:O_2 = 0.125$.

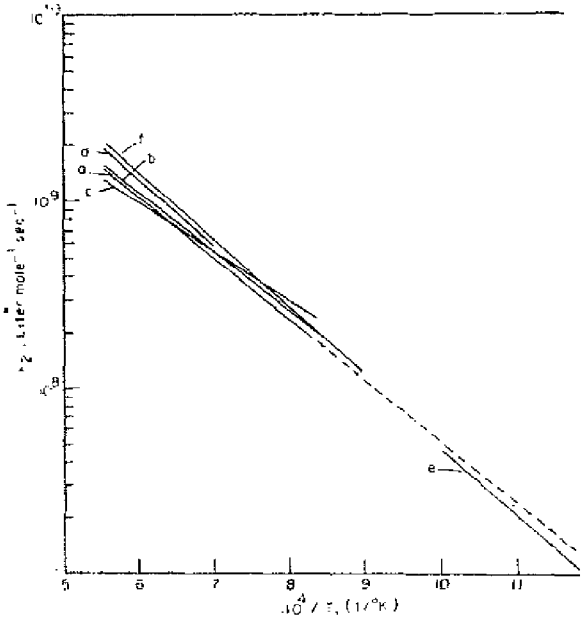

Figure 5. Rate coefficients for reaction II: *a*, this report; *b*, Gutman et al. [12]; *c*, Schott [13]; *d*, Browne et al. [14]; *e*, Kurzius and Boudart [15]; *f*, Leeds report [16].

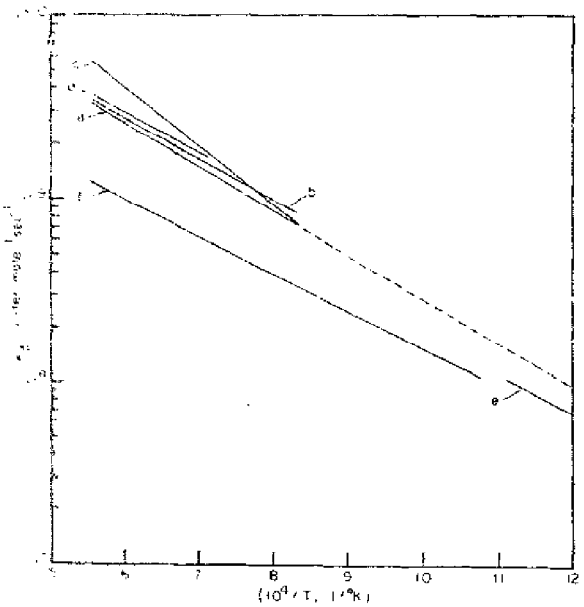

Figure 6. Rate coefficients for reaction III: *a*, this report; *b*, Gutman et al. [12]; *c*, Schott [13]; *d*, Browne et al. [14]; *e*, Westenberg and de Haas [17]; *f*, Leeds report [18].

5 are plotted in Fig. 5 and 6, respectively, together with some of the more recent expressions reported by others.

Gutman et al. [12] obtained data on reaction II by monitoring behind a reflected shock the oxygen atom increase during the induction period of the H_2-O_2 reaction. They report the expression

$$k_2 = 9.54 \times 10^{10} \exp\left(-\frac{14700}{RT}\right) \text{ liter mole}^{-1} \text{ sec}^{-1}$$

over the temperature range 975–2060°K. Our value for k_2 is about 10% smaller at 1200°K and 5% smaller at 1800°K than the values given by their expression.

Schott [13] in a similar study reports the expression

$$k_2 = 8.6 \times 10^{8} \exp\left[-\frac{12300}{R}\left(\frac{1}{T}-\frac{1}{1600}\right)\right] \text{ liter mole}^{-1} \text{ sec}^{-1}$$

which gives values that are about 10% larger than those obtained with Eq. 4 at 1200°K and 10% smaller at 1800°K.

In another shock-tube study Browne et al [14] obtained the expression

$$k_2 = 2 \times 10^{11} \exp\left(-\frac{16700}{RT}\right) \text{ liter mole}^{-1} \text{ sec}^{-1}$$

for the temperature range 1400–3000°K by matching analytic and experimental density profiles. Equation 4 gives values which are in good agreement with theirs at the lower temperatures; however, at 1800°K our k_2 is about 30% smaller than theirs.

From a study of the lower explosion limits in H_2-O_2-Ar mixtures in the temperature range 800–1000°K, Kurzius and Boudart [15] recently reported the expression

$$k_2 = 1.64 \times 10^{11} \exp\left(-\frac{16200}{RT}\right) \text{ liter mole}^{-1} \text{ sec}^{-1}$$

which is in good agreement with other low-temperature data [15]. Our extrapolated values are about 25% larger than the values given by the expression of Kurzius and Boudart.

In comparison with the expression

$$k_2 = 2.24 \times 10^{11} \exp\left(-\frac{10800}{RT}\right) \text{ liter mole}^{-1} \text{ sec}^{-1}$$

recommended by the Leeds report [16] Eq. 4 gives values that are about 10% smaller at 1200 K and 25% smaller at 1800°K; however, this difference is well within the error limits of ±50% suggested by Baulch et al.

As the above comparisons indicate, Eq. 4 is in good agreement with other data.

It should be pointed out that the expression for k_2 obtained in this study has an activation energy (15.02 kcal mole^{-1}) that is lower than the endothermicity of the reaction (15.94 kcal mole^{-1} at 1500°K). However, we feel that this apparent discrepancy is reconcilable within the probable errors of the present study. With the estimated error in k_2 of ±15% this could amount to an error in the activation energy of about ±1.2 kcal mole^{-1}.

For reaction III Gutman et al. [12] report the expression

$$k_3 = 6.07 \times 10^{10} \exp\left(-\frac{10200}{RT}\right) \text{ liter mole}^{-1} \text{ sec}^{-1}$$

which was derived from an assumed activation energy of 10.2 kcal mole^{-1} and a mean value of 1.98×10^9 liter mole^{-1} sec^{-1} at 1500°K. Equation 5 is in good agreement with this expression, at least over the temperature range 1200–1800°K. At 1500°K Eq. 5 gives the value 1.8×10^9 liter mole^{-1} sec^{-1}.

Browne et al. [14] recently reported the expression

$$k_3 = 6 \times 10^{10} \exp\left(-\frac{10000}{RT}\right) \text{ liter mole}^{-1} \text{ sec}^{-1}$$

for the temperature range 1400–3000°K, which gives values that are about 10–20% larger than those given by Eq. 5.

Schott [13] in his study of the H_2-O_2 reaction did not evaluate an expression for k_3 but instead evaluated the expression

$$k_1 k_3 = 1.5 \times 10^{19} \exp\left[-\frac{20000}{R}\left(\frac{1}{T} - \frac{1}{1600}\right)\right] \text{ liter}^2 \text{ mole}^{-2} \text{ sec}^{-2}$$

Setting $k_1 = 2.3 \times 10^{10} \exp(-5200/RT)$ liter mole^{-1} sec^{-1} Schott's expression gave k_3 values that were generally much larger than those from Eq. 5 (see Fig. 6).

In the low-temperature region Westenberg and de Haas [17] report the expression

$$k_3 = 3.2 \times 10^{10} \exp\left(-\frac{10200}{RT}\right) \text{ liter mole}^{-1} \text{ sec}^{-1}$$

for the temperature range 500–900°K, which is in good agreement with other low-temperature data. Equation 5 gives extrapolated values that are about 40% higher.

The Leeds [18] recommendation for k_3, which appears to be based on data below 1000°K, is smaller by about a factor of 2 than Eq. 5 in the temperature range 1200–1800°K.

Conclusions

From measurements of the exponential growth of the OH concentration in shocked H_2-O_2-Ar mixtures, rate coefficient data have been obtained for the chain-branching reactions $H + O_2 \xrightarrow{k_2} OH + O$ and $O + H_2 \xrightarrow{k_3} OH + H$ over the temperature range 1200–1800°K. The rate coefficient expressions are given by

$$k_2 = 9.9 \times 10^{10} \exp\left(-\frac{15020}{RT}\right)$$

and

$$k_3 = 7.5 \times 10^{10} \exp\left(-\frac{11100}{RT}\right) \text{ liter mole}^{-1} \text{ sec}^{-1}$$

The k_2 values are in reasonably good agreement with recent values reported in the literature for the temperature range 900–1800°K. The values for k_3 are in fair agreement with some recent shock-tube data over the temperature range 1200–1800°K, but are generally higher than the values reported in the literature [18].

The authors wish to thank Dr. Robert Rogowski for many helpful discussions regarding the analysis of the data and Mr. Hollie Ozment for assistance in performing the experiments.

References

1. SCHOTT, G. L., and KINSEY, J. L., *J. Chem. Phys.*, **29**, 1177 (1958).
2. SKINNER, G. B., and RINGROSE, G. H., *J. Chem. Phys.*, **42**, 2190 (1965).
3. ASAIBA, T., GARDINER, W. C., Jr., and STUBGEMAN, R. F., *Tenth Symposium (International) on Combustion*, p. 295. The Combustion Institute: Pittsburgh (1965).
4. MIYAMA, H., and TAKEYAMA, T., *J. Chem. Phys.*, **41**, 2287 (1964).
5. BELLES, F. E., and LAUVER, M. R., *J. Chem. Phys.*, **40**, 415 (1964).
6. KONDRAT'EV, V. N., *Chemical Kinetics of Gas Reactions*, p. 615. Pergamon: New York (1964).
7. BROKAW, R. S., *Tenth Symposium (International) on Combustion*, p. 269. The Combustion Institute, Pittsburgh (1965).
8. PENNER, S. S., *Quantitative Molecular Spectroscopy and Gas Emissivities*, p. 46. Addison-Wesley: Reading, Mass. (1959).
9. HOUGHTON, W. M., and JACHIMOWSKI, C. J., *Appl. Opt.*, **9**, 329 (1970).
10. MARGENAU, H., and MURPHY, G. M., *The Mathematics of Physics and Chemistry*, p. 517. D. Van Nostrand. Princeton, N. J. (1956).
11. DIXON-LEWIS, G., WILSON, W. E., and WESTENBERG, A. A., *J. Chem. Phys.*, **44**, 2877 (1966).
12. GUTMAN, D., HARDWIDGE, E. A., DOUGHERTY, F. A., and LUTZ, R. W., *J. Chem. Phys.*, **47**, 4400 (1967).
13. SCHOTT, G. L., *Twelfth Symposium (International) on Combustion*, p. 569. The Combustion Institute: Pittsburgh (1969).
14. BROWNE, W. G., WHITE, D. R., and SMOKLER, G. R., *Twelfth Symposium (International) on Combustion*, p. 557. The Combustion Institute: Pittsburgh (1969).
15. KURZIUS, S. C., and BOUDART, M., *Combustion & Flame*, **12**, 477 (1968).
16. BAULCH, D. L., DRYSDALE, D. D., and LLOYD, A. C., "High Temperature Reaction Rate Data," Report 3, School of Chemistry, The University, Leeds 2, England (November 1968).
17. WESTENBERG, A. A., and DE HASS, N., *J. Chem. Phys.*, **50**, 2512 (1969).
18. BAULCH, D. L., DRYSDALE, D. D., and LLOYD, A. C., "High Temperature Reaction Rate Data," Report 2, School of Chemistry, The University, Leeds 2, England (November 1968).

(Received March 1970; revised July 1970)